

****Volume Title****

*ASP Conference Series, Vol. **Volume Number***

****Author****

© ****Copyright Year**** *Astronomical Society of the Pacific*

Photometric properties of carbon stars in the Small Magellanic Cloud

G. C. Sloan¹, E. Lagadec², K. E. Kraemer³, M. L. Boyer⁴, S. Srinivasan⁵, I. McDonald⁶, and A. A. Zijlstra⁶

¹*Center for Radiophysics and Space Sciences, Cornell University, Ithaca, NY 14853-6081, USA*

²*Laboratoire Lagrange, UMR 7293, Univ. Nice Sophia-Antipolis, CNRS, Observatoire de la Côte d’Azur, 06300, Nice, France*

³*Institute for Scientific Research, Boston College, Chestnut Hill, MA 02467, USA*

⁴*Observational Cosmology Lab, Code 665, NASA Goddard Space Flight Center, Greenbelt, MD 20771, USA*

⁵*Academia Sinica Institute of Astronomy and Astrophysics, Taiwan University, Roosevelt Road, Taipei 10617, Taiwan*

⁶*Jodrell Bank Centre for Astrophysics, Alan Turing Building, Manchester, M13 9PL, UK*

Abstract.

The Optical Gravitational Lensing Experiment identified over 1,800 carbon-rich Mira and semi-regular variables in the Small Magellanic Cloud. Multi-epoch infrared photometry reveals that the semi-regulars and Miras follow different sequences in color-color space when using colors sensitive to molecular absorption bands. The dustiest Miras have the strongest pulsation amplitudes and longest periods. Efforts to determine bolometric magnitudes reveal possible systematic errors with published bolometric corrections.

The Optical Gravitational Lensing Experiment (OGLE) has surveyed the Small Magellanic Cloud (SMC) for variables and transients. The OGLE-III experiment discovered over 4,500 Mira and semi-regular variables (SRVs). Carbon stars account for 315 of the Miras and 1,488 of the semi-regular variables (Soszyński et al. 2011).

To investigate the infrared (IR) photometric properties of the carbon-rich long-period variables (LPVs), we have searched multiple archival databases to generate a time-averaged spectral energy distribution for each source. The OGLE survey provides mean *V* and *I* data. The Two-Micron All-Sky Survey (2MASS), the deeper 2MASS 6x survey, and the Deep Near-Infrared Survey of the Southern Sky (DENIS) provide three or more epochs at *J* and *K* and two at *H* (Skrutskie et al. 2006; Cioni et al. 2000). The SAGE-SMC survey (Surveying the Agents of Galactic Evolution), in combination with the S³MC survey (*Spitzer* Survey of the SMC), provides three epochs at 3.6, 4.5, 5.8, 8.0, and 24 μ m in the core of the SMC and two throughout the galaxy (Gordon et al. 2011; Bolatto et al. 2007). We have also turned to the Wide-field Infrared Survey

Experiment (WISE) for additional temporal coverage at 3.4 and 4.6 μm (Wright et al. 2010), which we use in conjunction with the *Spitzer* data at 3.6 and 4.5 μm .

Our presentation in Vienna considered both the Large and Small Magellanic Clouds, but here, due to space restrictions, we focus on just the SMC. The results for the two galaxies are generally very similar.

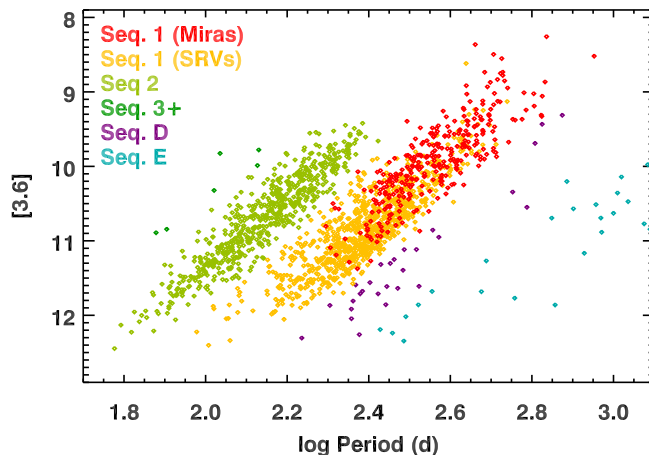


Figure 1. The period-luminosity diagram for carbon-rich Miras and SRVs, color-coded by pulsational sequence (following the nomenclature of Fraser et al. 2008). Fundamental-mode pulsators on the Sequence 1 are coded red and orange depending on whether the OGLE survey identified them as Miras or SRVs.

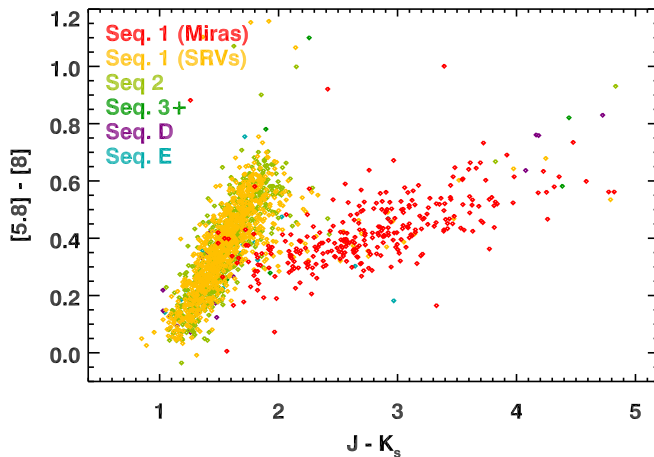


Figure 2. In the $[5.8]-[8]$ vs. $J-K_s$ plane, nearly all semi-regulars follow a blue sequence with $J-K_s \lesssim 2$, while Miras dominate the redder sequence.

The OGLE-III survey provides three periods and amplitudes. We chose the first period and amplitude corresponding to Sequence 1-4 (adopting the nomenclature of Fraser et al. 2008). Figure 1 shows how most of the Miras and SRVs fall along Sequences 1 and 2, which are the fundamental pulsation mode and the first overtone,

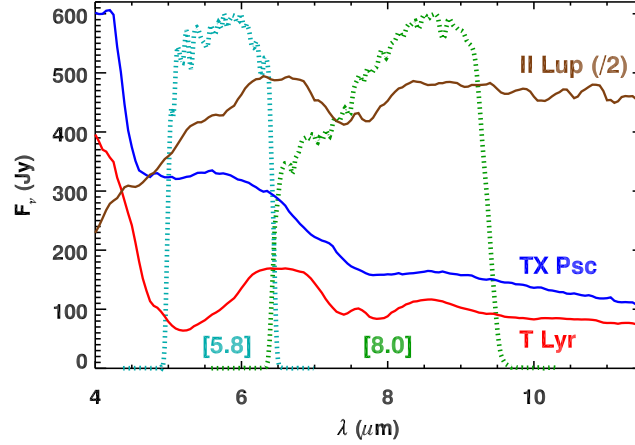


Figure 3. The 5.8 and 8 μm bandpasses on the Infrared Array Camera (IRAC) on *Spitzer* plotted over spectra from the spectral atlas from the Short-Wavelength Spectrometer (SWS) on the *Infrared Space Observatory* (Sloan et al. 2003). T Lyr has a redder [5.8]–[8] color than TX Psc because of the deep absorption from C_3 at $\sim 5 \mu\text{m}$. II Lup is red because of its thick dust shell.

respectively (Wood & Sebo 1996). These sequences are the basis for the color-coding in Figures 1 and 2, with different colors to distinguish the Miras and SRVs on Sequence 1. The OGLE-III survey separates these two variability classes at an I -band amplitude of 0.8 mag (peak-to-peak). Figure 2 shows how [5.8]–[8] and $J-K_s$ colors separate the Miras and SRVs relatively cleanly. Most of the SRVs fall on a sequence where [5.8]–[8] increases quickly as $J-K_s$ increases, while most of the Miras fall on a sequence which is much redder in $J-K_s$ and has a much shallower slope.

Figure 3 shows how the infrared spectra lead to two sequences, which we will refer to as the SRV and Mira sequences. Redder [5.8]–[8] colors on the SRV sequence, represented by TX Psc and T Lyr, result from increasing absorption from C_3 at 4.5–6.0 μm , which affects the 5.8 μm bandpass. On the Mira sequence, represented by II Lup, redder colors result from increasing dust opacity.

For the remaining figures in this contribution, we have adopted the color-coding defined in Figure 4, with blue to green depicting the SRV sequence in order of increasing [5.8]–[8] color and yellow to red tracking increasing $J-K_s$ color along the Mira sequence. Figure 5 shows how these different groups map into pulsation amplitude at I and pulsation period. These groups improve on the boundary between Miras and SRVs adopted by the OGLE-III survey (at $\Delta I = 0.8$ mag). The Mira sequence is associated with the larger amplitudes, and within this group, the dustier sources have the longest periods. This figure clearly links pulsation and dust production.

Comparing the bolometric magnitude and pulsation to theoretical evolutionary tracks allows one to estimate initial masses, but determining the bolometric magnitude from the available photometry is non-trivial. In Figure 6, the bolometric magnitudes are determined with bolometric corrections (BCs) based on $J-K_s$ (Whitelock et al. 2006). Two problems are apparent. The reddest and bluest sources on the SRV sequence have separated from each other, on both the overtone and fundamental modes. We call this problem the *blue slip*. It should be noted that we have applied the BC below the recommended limit of $J-K_s \gtrsim 1.5$. On the fundamental mode, another problem which we

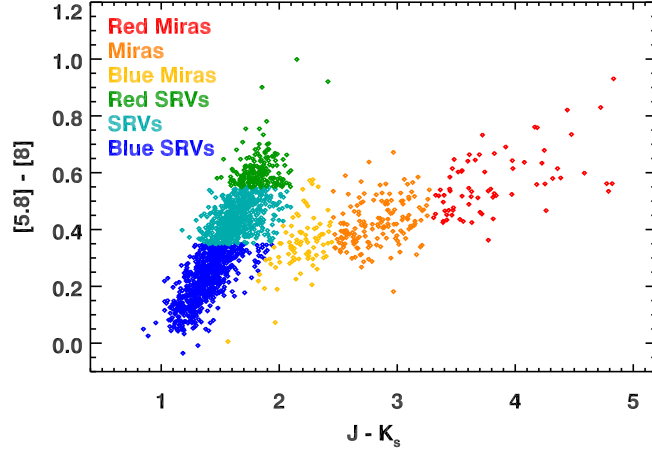


Figure 4. Carbon-rich Miras and SRVs in the SMC, color-coded by position along the SRV and Mira sequences in $[5.8]-[8]$ vs. $J-K_s$ space. Both sequences are divided into three strips to define the six groups.

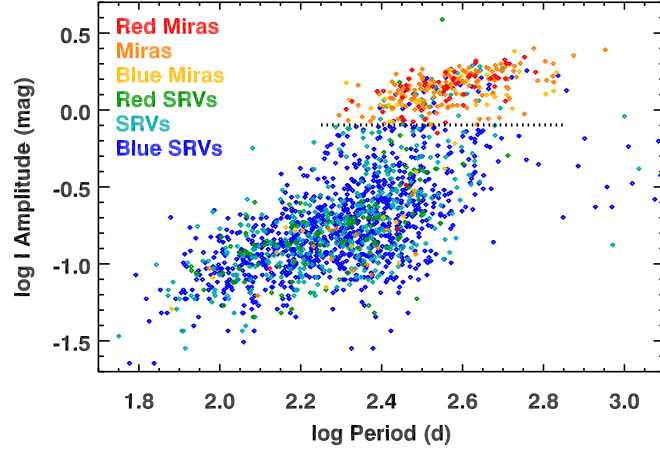


Figure 5. Pulsational amplitude at I vs. period, color-coded as in Fig. 3. The sources on the Mira sequence have larger amplitudes, and for these amplitudes, the reddest Miras have the longest periods. The horizontal dashed line shows the amplitude boundary of 0.80 mag between Miras and SRVs in the OGLE-III survey.

describe as the *red droop* has shifted the apparent bolometric magnitudes of the reddest sources well below the expected P-L relation. Using BCs from other authors produces results similar to those illustrated here.

Figure 7 shows that BCs based on $K-L$ reduce both the *blue slip* and *red droop*, but not entirely in either case. (We have treated L , $[3.4]$, and $[3.6]$ as equivalent here.) These problems probably arise from the BCs and are not intrinsic to the stars themselves. The need for improved means of determining bolometric magnitudes is readily apparent.

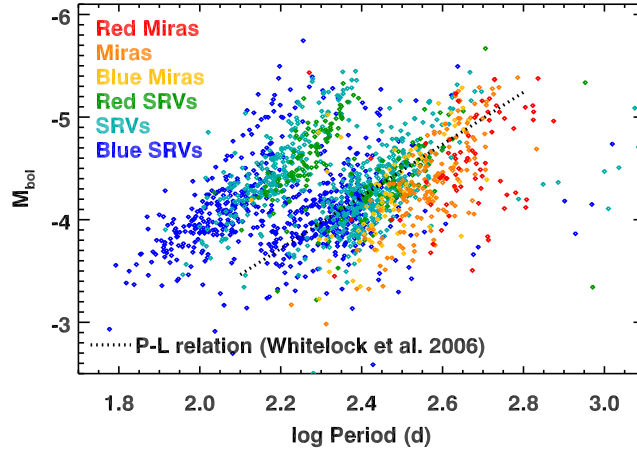


Figure 6. The period-luminosity diagram for the SMC after making $J-K_s$ -based bolometric corrections, color-coded as defined in Fig. 4. With these BCs, sources from different parts of the Mira and SRV sequences shift away from each other in P-L space, creating the *blue slip* and *red droop*.

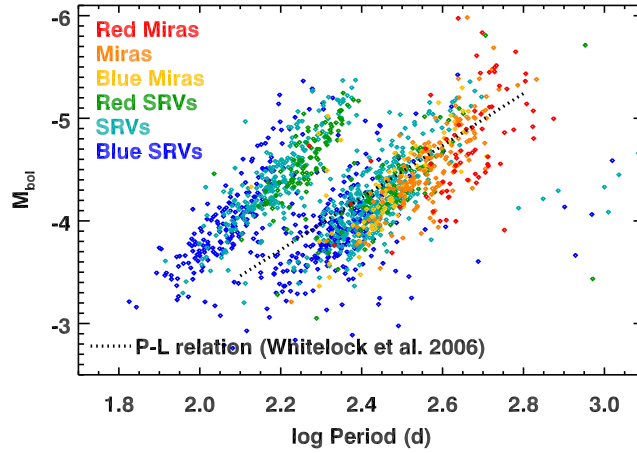


Figure 7. Bolometric corrections based on $K-L$ reduce both the *blue slip* and the *red droop*, but they do not eliminate them completely.

- Fraser, O. J., Hawley, S. L., & Cook, K. H. 2008, *AJ*, 136, 1242
 Gordon, K. D., Meixner, M., Meade, M. R., et al. 2011, *AJ*, 142, 102
 Skrutskie, M. F., Cutri, R. M., Stiening, R., et al. 2006, *AJ*, 131, 1163
 Sloan, G. C., Kraemer, K. E., Price, S. D., & Shipman, R. F. 2003, *ApJS*, 147, 379
 Soszyński, I., Udalski, A., Szymański, M. K., et al. 2011, *Act. Astron.* 61, 217
 Whitelock, P. A., Feast, M. W., Marang, F., & Groenewegen, M. A. T. 2006, *MNRAS*, 369, 751
 Wood, P. R., & Sebo, K. M. 1996, *MNRAS*, 282, 958
 Wright, E. L., Eisenhardt, P. R. M., Mainzer, A. K., et al. 2010, *AJ*, 140, 1868